The First Measurements of Galaxy Clustering from IRAC Data of the Spitzer First Look Survey

Fan Fang, David L. Shupe, Gillian Wilson, Mark Lacy, Dario Fadda, Tom Jarrett[1], Frank Masci, P. N. Appleton, Lee Armus, Scott Chapman, Philip I. Choi, D. T. Frayer, Ingolf Heinrichsen, George Helou, Myungshin Im[2], Francine R. Marleau, B. T. Soifer, Gordon K. Squires, L. J. Storrie-Lombardi, Jason Surace, Harry I. Teplitz, Lin Yan

Spitzer Science Center, Caltech 314-6, Pasadena, CA 91125

ABSTRACT

We present the first results of the angular auto-correlation function of the galaxies detected by the Infrared Array Camera (IRAC) instrument in the First Look Survey (FLS) of the Spitzer Space Telescope. We detect significant signals of galaxy clustering within the survey area. The angular auto-correlation function of the galaxies detected in each of the four IRAC instrument channels is consistent with a power-law form $w(\theta) = A\theta^{1-\gamma}$ out to $\theta = 0.2^\circ$, with the slope ranging from $\gamma = 1.5$ to 1.8. We estimate the correlation amplitudes A to be 2.95×10^{-3}, 2.03×10^{-3}, 4.53×10^{-3}, and 2.34×10^{-3} at $\theta = 1^\circ$ for galaxies detected in the IRAC 3.6μm, 4.5μm, 5.8μm, and 8.0μm instrument channels, respectively. We compare our measurements at 3.6μm with the previous K-band measurements, and discuss the implications of these results.

Subject headings: infrared: galaxies – large-scale structure of universe

1. Introduction

Since the early photographic-plate surveys the angular 2-point correlation function has been used to first characterize the galaxy spatial distribution in a catalog (Groth & Peebles 1977). Combined with selection function models in the third dimension these characterizations can yield information of the galaxy distribution in space and time, providing important clues to how structures form and evolve.

[1]Infrared Processing and Analysis Center, Caltech 100-22, Pasadena, CA 91125

[2]School of Earth and Environmental Sciences, Seoul National University, Seoul, S. Korea

So far these statistical characterizations have been established for galaxies in wavelengths that are systematically probed to various sensitivity levels. At the near-infrared K-band, for example, the angular galaxy clustering has been extensively measured to various depths (Baugh et al. 1996; Roche et al. 1998; Roche et al. 1999; Roche et al. 2002; Roche et al. 2003; Daddi et al. 2000; Kummel & Wagner 2000; McCracken et al. 2000; Maller et al. 2003) It is interesting to compare these K-band measurements with the ones from the Infrared Array Camera (IRAC) onboard the Spitzer Space telescope, since they detect the same population of evolved star-forming systems, as the rest-frame K-wavelength shifts into the IRAC wavelengths at higher redshifts.

The First Look Survey (FLS) using IRAC opens up new windows in near to mid-infrared wavelengths and detects galaxies to great sensitivity levels for the first time. The large survey area (4 square degrees) yields data fit for such statistical characterizations.

We report our results in this paper. In the next section we describe the data and outline our reduction procedure. In Section 3 we present our results. We compare our results with those in the K-band and discuss their implications in Section 4.

2. Data

The First Look Survey is designed to provide a characteristic first-look at the mid-infrared sky to sensitivities that are two orders of magnitudes deeper than previous large-area surveys. The Infrared Array Camera (IRAC) uses four imaging detectors with passbands centered at wavelengths 3.6 μm, 4.5 μm, 5.8 μm, and 8.0 μm. The IRAC FLS survey provides a uniform coverage of a 4 square-degree field centered at $RA = 17^h18^m$, $Dec = 59°30'$ with a total 60-second exposure time for each pixel in the 256×256 arrays.

Our starting point is the source catalog for each IRAC channel (Lacy et al. 2004). In brief the Basic Calibrated Data of each IRAC channel was mosaicked for the entire FLS field, source-extracted using SExtractor involving mask and coverage images, and spurious sources removed. Aperture corrections were applied to aperture fluxes in the source lists.

To separate stars from the source lists, we use the FLS R-band catalog (Fadda et al. 2004) covering the same field. We perform a bandmerge with the R-catalog for each source list of the IRAC channels. Since no apparent decrease of star counts up to R=24 in the R-catalog is found (Fadda et al. 2004), we delete IRAC sources with R-band stellarity index greater than 0.9 up to R=24. We verify the validity of this criteria by establishing histograms of the R-band stellarity index in several magnitude bins, which show that the stellarity index peaks at > 0.9 down to $R > 24$ (Hatziminaoglou 2004).

We band-merge the four IRAC source lists to study the source distribution in the IRAC color-space before and after the de-contamination of stars brighter than R=24. We verify that the star de-contamination significantly reduces the concentration of sources at colors corresponding to the Rayleigh-Jeans flux ratios at IRAC wavelengths. However, the process also deletes a population of red sources with high R-band stellarity, some of which may correspond to AGN at high redshifts (Lacy et al. 2004). We then follow the same color criteria used in **(author?)** (Lacy et al. 2004) and place these sources back to our IRAC source lists. The number of sources thus classified as stars and dropped from the samples are 27,049, 21,365, 8,176, and 5,144 for the 3.6μm, 4.5μm, 5.8μm, and 8.0μm, respectively.

We estimate the quality of the star/galaxy separation by comparing the resulting 3.6μm star and galaxy counts with the existing models. A star-counts model from the 2MASS survey (Jarrett 2004) predicts a total of 27,583 stars to the 5-σ sensitivity level in the validated 3.6μm area, slightly higher than 27,049 stars from our separation. The remaining contamination, mostly by fainter stars, is less than 2.5%. We establish flux-limited samples to avoid selection effects (see below) at 15-σ. At these sensitivities the remaining contamination becomes negligible. We then establish galaxy source counts based on the decontaminated 3.6μm source list, which fits well to the deep K-band source-counts after correction based on average galaxy color (Wilson et al. 2004; Jarrett 2004). The comparisons of the 3.6μm source counts with the models show the general quality of our star/galaxy separation procedures.

To this point the sources in our list are selected in regions of slightly different IRAC coverages. To eliminate the bias of source selection across the field caused by any non-uniform survey coverage, we establish our final source lists to include sources above 15-σ sensitivity levels. Table 1 lists the flux-limits and number of sources in these source lists.

3. Results

The angular auto-correlation function, $w(\theta)$, measures the excess numbers of pairs of galaxies in a single catalog as a function of angular separation compared to those in a random distribution. We have calculated the angular correlation function using the **(author?)** (Landy & Szalay 1993) estimator,

$$w(\theta) = \frac{DD - 2DR + RR}{RR}. \quad (1)$$

Here DD, DR, and RR are normalized pair-counts in a given angular separation of the data-data, data-random, and random-random sources, respectively. For each IRAC-channel

data, we generate 10 realizations of random sources using the mask and coverage files that our source lists are based on, to ensure similar source selection. The number of the random points generated in each realization is approximately identical to the number of galaxies in an IRAC source list.

The correlation signal is calculated in each angular separation range after binning the data. The uncertainty across different angular bins are not independent but correlated. To better estimate the uncertainty in our measurements, we use the Jackknife analysis (Scranton et al. 2002; Maller et al. 2003) to calculate the uncertainties for each angular bin by dividing the survey area into 20 tiles. We calculate the correlation each time by removing sources in a tile and obtained 20 correlation estimates based on which the uncertainties of the correlation signal are estimated. Due to the sample size we perform the Jackknife analysis for the 3.6μm and 4.5μm data only. For the 5.8μm and 8μm our sample sizes are not appropriate for the Jackknife analysis. We calculated Poisson errors in these cases $\delta w(\theta) = \sqrt{(1 + w(\theta))/DD}$ (Hewitt 1982). However we need to bear in mind that using Poisson uncertainites do not include the correlation noise between the angular bins and therefore may underestimate the total noise. A comparison between the power-law models fits (see below) of using Jackknife errors and Poisson errors in our 3.6μm and 4.5μm data shows that using Poisson errors can under-estimate the uncertainties in the amplitude by up to 50% while over-estimating the amplitude values by up to 22% in our cases.

Due to limited sample size the angular correlation calculated this way are known to be biased to lower values, and the so-called "Integral constraints" need to be estimated to correct for the bias. We calculate the integral constraints for our samples following **(author?)** (Roche & Eales 1999). The correlation amplitudes quoted in this paper are all corrected ones.

In Figure 1 we illustrate the angular correlation functions we measured at the four IRAC wave-bands. Comparing with random distributions, there are strong signals of galaxy clustering in the IRAC wavelengths. We find that the four auto-correlation functions are well-approximated by power-laws out to about 0.2°. The amplitude and slope of the correlation vary from band to band. We also plot by the solid lines in the Figure the single-power-law model for each of the measured correlation after corrections for integral constraint are made. Table 1 lists the parameters of the models.

4. Summary and Discussion

We have measured the angular 2-point auto-correlation function of galaxies in the FLS IRAC data. We find the the angular correlations in IRAC wavelengths are consistent with power-laws with varying slope and amplitude.

Old stellar populations contribute significantly to IRAC wavelengths. Galaxies dominated by these populations are mostly elliptical galaxies. Since these galaxies are known to cluster more strongly (Dressler 1980) than other types of galaxies where younger stellar populations dominate, we would expect to detect strong clustering in IRAC surveys. Our estimate of the correlation amplitude is higher than but marginally consistent with what is measured in the 3.6μm channel in the SWIRE Lockman and ELAIS N1 fields (Oliver et al. 2004), where a slightly steeper correlation slope is found.

For IRAC channels, especially at 3.6μm, the nearby K-band has extensive measurements of galaxy angular correlations to various depths. In Figure 2 we compare our full-sample measurement with various results from the K-band magnitude-limited samples in the recent literature. In order to make these comparisons, we use a fixed slope, $\gamma = 1.8$, to re-calculate the integral constraint and the correlation amplitude in our 3.6μm sample limited at 15-σ. The same fixed-slope has been used in most of the K-band measurements we compare with. We obtain an amplitude of $(6.81 \pm 1.00) \times 10^{-4}$. We use an average color of 1.1 (Oliver et al. 2004) to scale the K-magnitude limits in various measurements to the 3.6μm magnitude and flux. The Figure also shows the uncertainty of this color-scaling. Based on the Figure we conclude that our measurement is only marginally consistent with the K-band results from the various magnitude-limited samples. Our lower estimate of the correlation amplitude in the 3.6μm sample may indicate a different galaxy clustering property in this wavelength. However the difference is only marginal given the uncertainties in the color scaling. Since these wavelengths detect the same population of galaxies, and the rest-frame K-band sources also become IRAC detections at higher redshifts, there is good reason to believe that the galaxy clustering strengths in these wavelengths are close. Better SED models can resolve this as more IRAC data becomes available.

The galaxy angular correlation is a result of evolving spatial correlation scaled by a radial selection function integrated over redshifts. The radial selection function determines how galaxies are selected by a survey. They are formally related by the Limber equation (Limber 1953). Using a form of K-band selection function (Baugh et al. 1996) we perform the Limber integration of the 3.6μm measurement by assuming a spatial correlation amplitude of $r_0 = 4.2h^{-1}$Mpc and a slope of 1.8 (Oliver et al. 2004). In Figure 3 we plot the results. This places constraints on the median redshift of the sample we used. Depending on evolution models for galaxy clustering, the median redshift of the 3.6μm sample is ~ 0.42 if

clustering is fixed in proper coordinates, ~ 0.60 if clustering is fixed in comoving coordinates. Bracketed by these two evolution models, the exact value of the median redshift of the sample would be within this range if the selection function applies to the sample. However, so far we do not have enough information to determine if the form of the selection function used is appropriate, therefore the uncertainties in the median redshift estimate may be significant. The exact value shall be determined when redshifts of at least a sample representative of the distribution of sources in both depth and type are measured, at which point a reliable form of the spatial correlation and its evolution can be constrained.

To investigate the change of correlation function with flux, we establish two sub-samples at different flux limits for each IRAC channel and calculate the correlation function in these subsamples. The results are listed in Table 1. In all four IRAC passbands the correlation amplitudes decrease with increasing flux-limit values in the established subsamples. If we again assume the form of the selection function and the parameters of spatial correlations used in Figure 3, and that clustering is fixed in proper coordinates, we estimate that the median redshifts are 0.25 and 0.13, respectively for the 3.6μm "sub1" and "sub2" in Table 1. While we believe that the change of correlation amplitudes in subsamples of all IRAC channels has cosmological origin, we caution that the scaling of these to median redshifts using Figure 3 may lack accuracy, based on the above discussion. The results can be more fully interpreted when we have more complete information about the redshift distribution of the sources in these samples. We plan to pursue this as part of our future work.

We wish to thank an anonymous referee for help shaping up the final form of this paper. This work is based on observations made with the Spitzer Space Telescope, which is operated by the Jet Propulsion Laboratory (JPL), California Institute of Technology under NASA contract 1407. Support for this work was provided by NASA through JPL.

REFERENCES

Baugh, C. M., Gardner, J. P., Frenk, C. S., & Sharples, R. M. 1996, MNRAS, 283, L15.

Daddi, E. et al. 2000, A&A, 361, 535.

Fadda, D., Jannuzi, B., Ford, A., & Storrie-Lombardi, L. J. 2004, AJ, accepted.

Groth, E. J. & Peebles, P. J. E. 1977, ApJ, 217, 385.

Dressler, A. 1980, ApJ, 236, 351.

Hatziminaoglou, E. 2004, private communication.

Hewitt, P. C. 1982, MNRAS, 201, 867.

Jarrett, T. 2004, in preparation.

Kummel, M. W. & Wagner, S. J. 2000, A&A, 353, 867.

Lacy, M. et al. 2004, this issue.

Lacy, M. et al. 2004, in preparation.

Limber, D. N., 1953, ApJ, 117, 134.

Landy, S. D. & Szalay, A. S. 1993, ApJ, 412, 64.

Maller, A. H., McIntosh, D. H., Katz, N., & Weinberg, M. D. 2003, astro-ph/0304005.

McCracken, H. J., Shanks, T., Metcalfe, N., Fong, R., & Campos, A. 2000, MNRAS, 318, 913.

Oliver, S. et al. 2004, ApJ, this issue.

Roche, N., Eales, S., & Hippelein, H. 1998, MNRAS, 295, 946.

Roche, N. & Eales, S. A. 1999, MNRAS, 307, 703.

Roche, N., Eales, S. A., Hippelein, H., & Willott, C. J. 1999, MNRAS, 306, 538.

Roche, N., Almaini, O., Dunlop, J., Ivison, & Willott, C. J. 2002, MNRAS, 337, 1282.

Roche, N., Dunlop, J. & Almaini, O. 2003, MNRAS, 346, 803.

Scranton, R. et al. 2002, ApJ, 579, 48.

Wilson, G. et al. 2004, in preparation.

Fig. 1.— The angular 2-point auto-correlation functions measured for the IRAC channels. A power-law model $w(\theta) = A\theta^{1-\gamma}$ is shown by the lines, where corrections for the integral constraint are included. The Jackknife analysis is performed for the 3.6μm and 4.5μm, represented by the error bars. The uncertainties for 5.8μm and 8.0μm are Possion error which may underestimate the total error.

Fig. 2.— Our fixed-slope ($\gamma = 1.8$) estimate of the angular correlation amplitude at 3.6μm as compared with the K-band results from the literature. We scale the K-band magnitudes to the 3.6μm fluxes using an average color of 1.1. The horizontal error bar indicates the uncertainty of the color scaling for the K-band points. The fluxes represent the flux limit of a given sample. To be consistent, we only plot the result from the 15-σ flux-limited sample at 3.6μm.

Fig. 3.— Change of the angular correlation amplitude with the sample median redshift based on Limber integration. Here we use a form of selection function (Baugh et al. 1996) that has been studied in K-band surveys, and assumed a spatial correlation amplitude estimated from a 3.6μm SWIRE sample. The two evolution models for galaxy clustering along with the uncertainties from our angular correlation amplitude measurement places a contraint on the median redshift of the 3.6μm sample in the FLS survey.

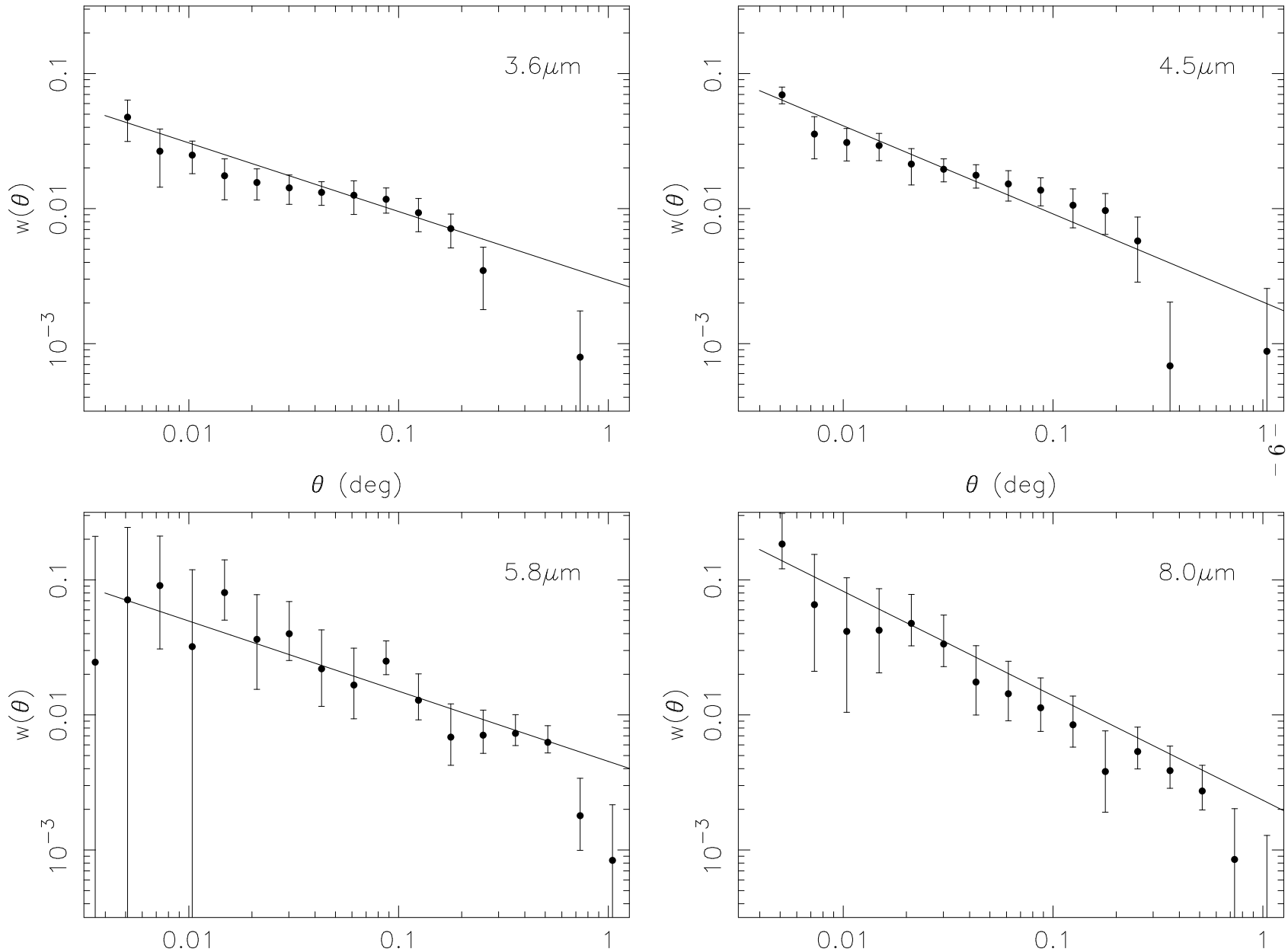
3.6μm
4.5μm
5.8μm
8.0μm
w(θ)
θ (deg)
0.1
0.01
10^−3
0.01
0.1
1

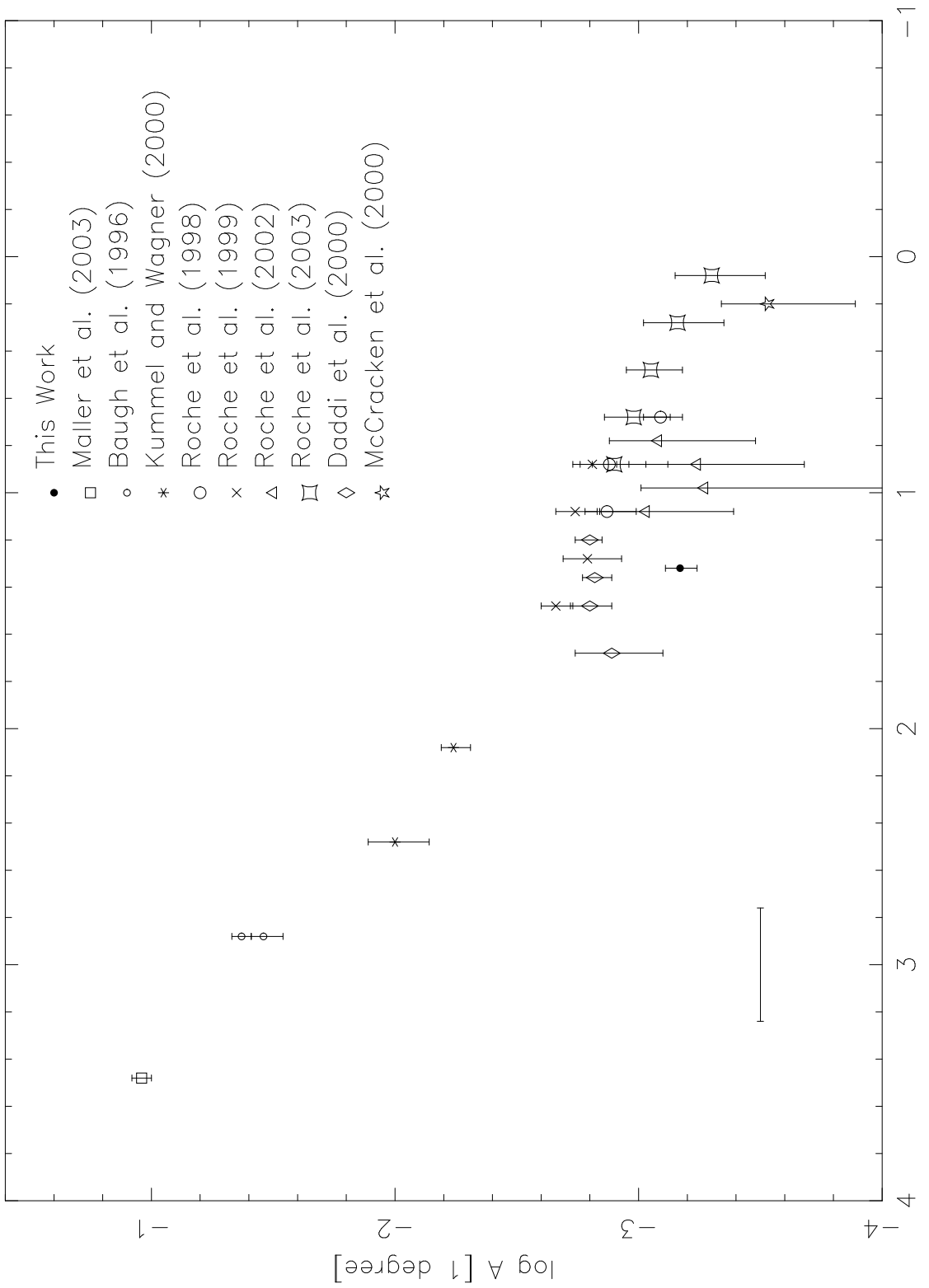
This Work
Maller et al. (2003)
Baugh et al. (1996)
Kummel and Wagner (2000)
Roche et al. (1998)
Roche et al. (1999)
Roche et al. (2002)
Roche et al. (2003)
Daddi et al. (2000)
McCracken et al. (2000)
log A [1 degree]
logf3.6 [μJy]
−1
−2
−3
−4
4
3
2
1
0
−1

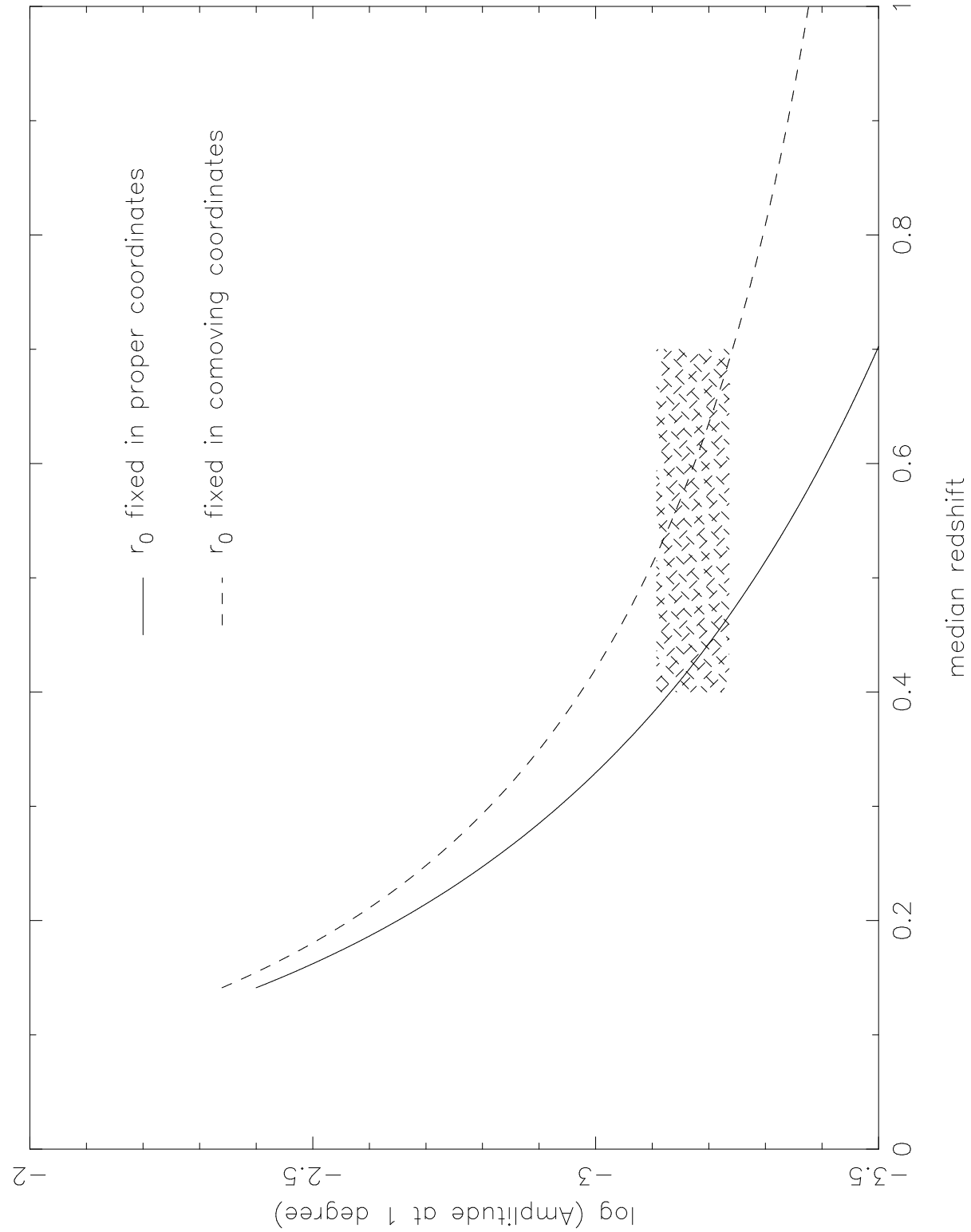
log (Amplitude at 1 degree)
−2
−2.5
−3
−3.5
0
0.2
0.4
0.6
0.8
1
median redshift
r_0 fixed in proper coordinates
r_0 fixed in comoving coordinates

Table 1. IRAC Samples and Angular Correlation functions[1]

Sample	flux limit	Galaxy Number	A (10^{-3})	γ	IC
3.6μm total	f_ν >18μJy	52790	2.95±1.84	1.51±0.32	1.14
3.6μm sub1	48μJy< f_ν <78μJy	9101	2.83±0.44	1.65±0.30	1.22
3.6μm sub2	78μJy< f_ν <120μJy	4354	4.33±0.11	1.79±0.29	1.31
4.5μm total	f_ν >21μJy	41936	2.03±0.45	1.65±0.30	1.22
4.5μm sub1	56μJy< f_ν <91μJy	5615	1.95±0.06	1.85±0.27	1.36
4.5μm sub2	91μJy< f_ν <140μJy	2498	9.87±1.10	1.56±0.29	1.17
5.8μm total	f_ν >135μJy	4207	4.53±1.10	1.52±0.26	1.15
5.8μm sub1	135μJy< f_ν <180μJy	1118	7.27±0.18	1.69±0.26	1.24
5.8μm sub2	180μJy< f_ν <270μJy	1108	11.40±0.30	1.64±0.26	1.21
8.0μm total	f_ν >96μJy	5721	2.34±0.13	1.77±0.28	1.30
8.0μm sub1	96μJy< f_ν <128μJy	1491	5.77±0.13	1.72±0.25	1.26
8.0μm sub2	128μJy< f_ν <192μJy	1577	8.23±0.30	1.64±0.25	1.21

[1]A power-law form $w(\theta) = A(\theta^{1-\gamma} - IC)$ is used to fit the data where IC is the integral constraint; θ is in degrees.